

Radiological characterization of building materials used in Malaysia and assessment of external and internal doses

Shittu Abdullahi^{1,3} · Aznan Fazli Ismail^{1,2} · Supian Samat²

Received: 11 July 2018 / Revised: 20 August 2018 / Accepted: 21 August 2018 / Published online: 13 February 2019
© China Science Publishing & Media Ltd. (Science Press), Shanghai Institute of Applied Physics, the Chinese Academy of Sciences, Chinese Nuclear Society and Springer Nature Singapore Pte Ltd. 2019

Abstract In this study, the activity concentrations of ^{226}Ra , ^{232}Th , ^{222}Rn , and ^{40}K , emanation fractions (P), equilibrium equivalent concentration (EEC), and mass exhalation rates (E_m) of radon released from building materials used in Malaysia were studied using gamma-ray spectrometer with HPGe detector. Radiological parameters [activity concentration index (ACI), indoor air-absorbed dose rate (D_{in}), annual effective dose (AED_{in}) from external and internal (E_{Rn}), soft tissues (H_{ST}) and lung (H_L), and effective dose equivalent (H_{eff})] were estimated to evaluate radiological hazards due to the use of these building materials: sand, cement, gravel, bricks, tiles, fly ash, white cement, and ceramic raw materials. The measured P , EEC, and E_m vary from 10 to 30%, 0.9 to 22 Bq m⁻³, and 33 to 674 mBq h⁻¹ kg⁻¹, respectively, while the calculated ACI and AED_{in} vary from 0.1 ± 0.01 to 2.1 ± 0.1 and 0.1 ± 0.01 to 2.4 ± 0.6 mSv y⁻¹, respectively. On the other hand, the internal annual effective dose ranges from 0.1 to 1.4 mSv y⁻¹. The estimated radiological risk

parameters were below the recommended maximum values, and radiological hazards associated with building materials under investigation are therefore negligible.

Keywords Indoor radon · Emanation fraction · Equilibrium equivalent concentration · Mass exhalation rate · Annual effective dose · Effective dose equivalent

1 Introduction

All materials present in the earth's crust contain some amount of natural radioactive elements. However, the most common Naturally Occurring Radioactive Materials (NORM) found in the environment are uranium (^{238}U), thorium (^{232}Th), and their progeny and isotope of potassium (^{40}K) [1–5]. Some materials such as industrial wastes and/or industrial by-products may contain high radioactive elements called Technologically Enhanced Naturally Occurring Radioactive Materials (TENORM). Radium (^{226}Ra) is mostly used as a reference radionuclide in the measurement of ^{238}U [5–7]. Most of the radiation exposure received by the general public from natural sources comes from the decay of ^{226}Ra which produces radon (^{222}Rn) gas and its decay products [8].

Radon is an immediate decay product of ^{226}Ra and is naturally occurring radioactive noble gas with important features: It is odorless and colorless, has about 3.8-day half-life, is present in the air and all building materials, and has four important immediate decay products including ^{218}Po , ^{214}Pb , ^{214}Bi , and ^{214}Po [3]. ^{222}Rn gas is the most important source of an indoor radiation exposure and accounts for about half of the worldwide background radiation dose received by human population [9, 10]. It

A part of this research was supported by Universiti Kebangsaan Malaysia and Lynas Advanced Material Plant under Grant Numbers GGPM-2017-084 and ST-2017-012, respectively.

✉ Aznan Fazli Ismail
aznan@ukm.edu.my

¹ Nuclear Science Program, Faculty of Science and Technology, Universiti Kebangsaan Malaysia (UKM), 43600 Bangi, Selangor, Malaysia

² Centre for Frontier Science, Faculty of Science and Technology, Universiti Kebangsaan Malaysia (UKM), 43600 Bangi, Selangor, Malaysia

³ Department of Physics, Faculty of Science, Gombe State University, P.M.B. 127, Gombe, Nigeria

emanates from rocks, soils, and building materials and is accumulated in enclosed places such as underground mines and houses [9–11]. Various international organizations such as the World Health Organization (WHO), International Commission on Radiological Protection (ICRP), International Atomic Energy Agency (IAEA), International Agency for Research on Cancer (IARC), and US National Toxicology Program (US NTP) have recognized ^{222}Rn as human carcinogen based on sufficient evidence [4, 11–14].

Long-term exposure to indoor ^{222}Rn concentrations could cause pathological effects and changes in the respiratory function and, thus, could increase the possibilities of developing lung cancer [15]. Some parts of ^{222}Rn decay products will also infiltrate into the blood from the lungs, thereby irradiating the whole human body [9]. The first cause of cancer mortality in the world is lung cancer. And smoking is the main cause of lung cancer, followed by indoor radon exposure. Furthermore, a statistics study showed that worldwide, about 10 to 25% of lung cancer cases occur among people with no history of smoking [16, 17].

Moreover, from a radiation viewpoint, lung cancer risks from the exposure of ^{222}Rn and its progeny are not the only concern: Other forms of cancer are also associated with radiation exposures such as X-radiation and gamma (γ) radiation. The exposure to the aforementioned radiations is strongly associated with leukemia and cancer of the thyroid, breast, and lung. The evidence was discovered at absorbed doses of less than 0.2 Gy. The tendency to develop these cancers depends on age. Other cancers such as the salivary glands, urinary bladder, stomach, ovary, colon, skin, and central nervous system are associated with high absorbed doses up to 1 Gy [12].

In Malaysia, cancer is one of the leading causes of death [18, 19]. According to a Malaysian National Cancer Registry (MNCR) report on cancer incidences from 2007 to 2011, a total number of 103,507 were recorded as new diagnosed cases of cancer and 45.2% of these cases were male while 54.8% cases were females. And, whereas colorectal, lung, nasopharynx, lymphoma, and prostate are common cancers among males, breast, colorectal, cervix uteri, ovary, and lung are common cancers among females [18, 19]. The report also showed that the number of deaths caused by cancer within this period is 64,275. And this cancer-caused death trend increased from 2007 to 2011. In Malaysia, lung cancer was ranked second and fifth most common cancers among males and females, respectively [18, 19]. Therefore, studying possible substances associated with cancer risks in Malaysia such as radiological health risks attributed to building materials and fractional contribution of each of the building materials to the exposure caused by inhalation of indoor radon and its progeny can be beneficial to local authorities and general public.

The aim of this study is to evaluate the level of natural radioactivity in Malaysian building materials and their associated radiological hazards to the human health by assessing external and internal doses resulted from the use of these materials under investigation.

2 Materials and methods

2.1 Sample preparation

The building materials under study are the common construction materials used by the Malaysian people. One hundred and two samples were sourced from various locations within Malaysia such as Selangor, Kuala Lumpur, Johor, Pahang, Terengganu, Kelantan, and Putrajaya. The selected building materials with sample identity (ID) in parentheses are tiles (1–40), red brick (41–45), cement brick (46–50), sand (51–60), cement (61–70), gravel (71–80), white cement (81–85), fly ash (86–90), feldspar (91–93), limestone (94–96), kaolin (97), pottery stone (98), clay (99–100), glaze (101), and talc (102). The samples were oven-dried at 105 °C for 48 h to ensure significant moisture content was removed, grinded, and then sieved using 500- μm -sized mesh. The grain size was carefully chosen to optimize the filling of the Marinelli beakers. They were then packed in a Marinelli beaker in three replicates, airtight sealed, labeled, weighed, and kept in a laboratory for 30 days to achieve radioactive secular equilibrium. The present study followed the standard sample preparation procedure as mentioned in the IAEA technical report series no. 295 [20].

2.2 Instrumentation

The gamma-ray spectroscopy consisted of a closed-end coaxial high-purity germanium (HPGe) detector, lead shielding, and electronics to process the signals produced by the detector (pulse sorter and related amplifiers). Additionally, it also consisted of readout devices such as a computer analyzer using Genie 2000 software to generate, display, and store the final gamma-ray spectrum. The 10-cm-thick cylindrical lead shield is coated with 1-mm tin and enclosed in a 1.6-mm copper HPGe detector capsule. The HPGe detector is mounted in a vacuum chamber inserted into a liquid nitrogen Dewar at a temperature of 77 K as a cooling medium for the system [21]. Other components include high voltage supply, depletion voltage, + 2500 V, recommended bias voltage + 3000 V, and pulse shaping time of 4 μs . The relative efficiency and full width at half maximum (FWHM) energy resolution at 1.33 MeV are 30% and 1.8 keV, respectively. The spectra data were analyzed using Genie 2000 software made by Canberra.

2.3 Detector calibration and measurement of natural radioactivity

The building materials are measured using gamma-ray spectroscopy employing a HPGe detector located within the Science Nuclear Building at the Universiti Kebangsaan, Malaysia. The absolute efficiency of the counting system was evaluated using a mixed standard source containing ^{22}Na , ^{57}Co , ^{60}Co , and ^{137}Cs . Also, the activities of the standard source at the time of study are 9.86 kBq, 0.03 kBq, 8.36 kBq, and 1.18 kBq for ^{22}Na , ^{57}Co , ^{60}Co , and ^{137}Cs , respectively. Routine background measurements were carried out before commencing the counting of the samples. Reference materials (International Atomic Energy Agency: IAEA-375 soil) of known activities of ^{226}Ra , ^{232}Th and ^{40}K natural radionuclides. The IAEA-375 soil was prepared in three replicates and counted several times prior to counting of the samples with a view to compare the measured activity concentrations with the known activity concentrations of the IAEA-375 soil. The activity concentrations of ^{226}Ra , ^{232}Th , and ^{40}K of the IAEA-375 soil are 20, 20.5, and 424 Bq kg^{-1} , respectively.

Each sample was prepared in three replicates and counted for 43,200 s. The acquisition of data and identification of radionuclides based on their gamma-ray energy peaks were carried out using Canberra Genie 2000 software. An empty Marinelli beaker was counted for 43,200 s to obtain the background spectrum. The analyzed results of the HPGe detector were printed, and the identification of radionuclides of each sample was performed by selecting the net peak area of specific known gamma-ray energy peaks. The gamma-ray energy peaks used for identifying ^{226}Ra and ^{232}Th are 1764.5 keV (^{214}Bi) and 2614.5 keV (^{208}Tl), respectively, while singly occurring ^{40}K was identified directly from its gamma-ray energy peak of 1461 keV. The activity concentration of individual radionuclides was calculated using Eq. (5) [5, 22]. The minimum detectable activity (MDA) was calculated based on Curie's derivation [23]. The average MDA for the counting time of 43,200 s was 6.2 ± 0.1 , 5.3 ± 0.1 , and 22.1 ± 0.2 Bq kg^{-1} for 1764.5, 2614.5, and 1461 keV, respectively.

3 Results and discussion

3.1 Determination of radon emanation fraction (P)

The measurement of radon emanation fraction was carried out using gamma-ray spectroscopy coupled with a high-purity germanium (HPGe) detector. The samples were sealed in a counting bottle, and emitted gamma rays from ^{214}Pb and/or ^{214}Bi were counted in an interval of 2 days

before and after achieving radioactive equilibrium between the ^{226}Ra and its progeny. Therefore, the samples were counted 25 times in 50 days; the goal for extending the days up to 50 is to ensure the secular equilibrium between the parent nuclide and their decay progenies is clearly observed as shown in Fig. 1. When the ^{222}Rn and its progeny are in secular equilibrium, then the activities of ^{222}Rn and its progeny are equal [24]. Moreover, the activity concentration of ^{226}Ra was also investigated from various building materials. The choice of this method is born out of two major advantages: nondestructive and indirect measurement through the decay products of the ^{226}Ra nuclide. Since only relative counts are needed, no calibration is required for this method [25].

The expression in Eq. (1) shows the change in the total radon concentration C_{Rn} (Bq m^{-3}) with respect to time t (s) in solid and gas phases enclosed in a container [26]:

$$\frac{dC_{\text{Rn}}}{dt} = \frac{E}{V} - \lambda C_{\text{Rn}} \quad (1)$$

It follows that

$$C_{\text{Rn}}(t) = \frac{E}{\lambda V} (1 - e^{-\lambda t}) + C_{\text{Rn}}(0)e^{-\lambda t} \quad (2)$$

Equation (4) was further deduced as:

$$N(t) = N_{\text{eq}}\{1 - e^{-\lambda t}\} + N_0e^{-\lambda t}, \quad (3)$$

where E (Bq s^{-1}) is the radon exhalation rate from the sample, V is the volume of the sample container or counting bottle, and λ (s^{-1}) is the radon decay constant. Integrating Eq. (1), the radon growth is presented in Eq. (2), where $C_{\text{Rn}}(0)$ is the radon concentration at $t = 0$. At this point, all radon atoms exist in the solid phase. In other words, all radon atoms are present in the mineral

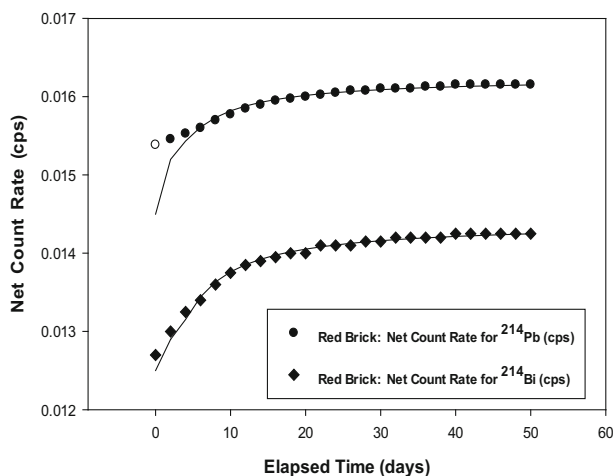


Fig. 1 An example of the growth of the radon daughters in a closed container for a grinded red brick sample. The solid lines indicate the fitting curves

grains. Whereas $N(t)$ is the net count rate of γ -rays, N_{eq} and N_0 are the net count rates at $t > 30$ days and $t = 0$, respectively. The net count rate N was obtained by fitting a series of N_{eq} and N_0 to Eq. (3). Equation (3) was used to determine the growth of ^{222}Rn decay daughters in a closed counting container. An example of measured data and fitting curves is shown in Fig. 1. It could be observed that the fitting was successful. Hence, the radon emanation fraction P (%) was calculated using Eq. (4) [25, 26]:

$$P = \frac{N_{\text{eq}} - N_0}{N_{\text{eq}}} \times 100 \quad (4)$$

The radon emanation fraction from six different building materials is measured and presented in Fig. 2 with values ranging from $10 \pm 0.4\%$ to $30 \pm 0.4\%$. The reported high values of cement brick and sand suggest that the radium contents in these materials are concentrated near the grain surface. Another possible factor is cracks on the surface of the grain, which may be from the previous radioactive decays and weathering effects: It can affect the surface area of the grain and subsequently increase the radon emanation fraction [25].

The International Atomic Energy Agency (IAEA) reported the radon emanation fraction of natural materials such as uranium mine and mill tailings, rocks, soils, and minerals ranges from 10 to 30% with high values reported for rocks, soils, and mill tailings, whereas low values less than 10% were reported for fly ash and minerals [25]. Sahoo et al. [27] reported an emanation fraction from Indian building materials using alphaguard, a continuous radon monitor, and their results range from 0.1 to 20.8% with maximum and minimum reported values in lime and vitrified tile, respectively [27]. UNSCEAR [28] provided a representative value of 20% for soil with a range of 1 to 80%. Martino [29] reported radon emanation fraction of soils using an electrostatic collector coupled to a silicon detector, and his results ranged from 6 to 60% [29].

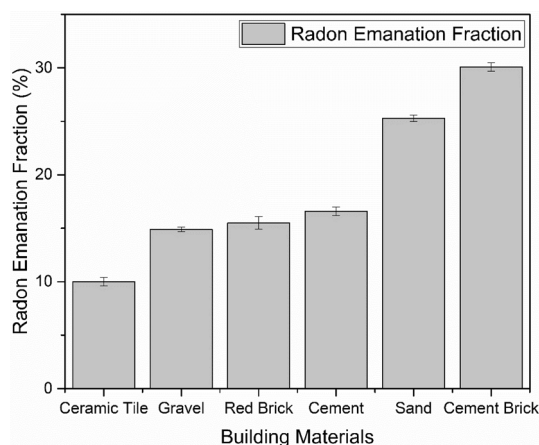


Fig. 2 Radon emanation fraction of various building materials

Bossew [30] reported the radon emanation fraction of building materials, soil, and rock using activated charcoal, and his results ranged from 0.6 to 29.5%, respectively. These reported findings are in accordance with the results of the present study.

3.2 Natural radioactivity and indoor radon concentration

The individual activity concentration (C_i) is calculated using Eq. (5) [5, 22]:

$$C_i = \frac{M_{\text{ref}} \times A_s}{M_s \times A_{\text{ref}}} \times C_{\text{ref}}, \quad (5)$$

where C_{ref} is the activity concentration of reference materials, M_s and M_{ref} are the mass of the sample (kg) and reference materials, respectively, and A_s and A_{ref} are the activity (cps) of sample and reference materials, respectively.

Radon is the most important natural radionuclide in the indoor environment. Generally, only a few people are exposed to high ^{222}Rn and the majority of the lung cancers are caused by low and moderate ^{222}Rn exposure [11]. All building materials contain some natural radionuclides such as ^{238}U and ^{232}Th and their decay series and singly occurring ^{40}K [1, 11]. The concentrations of natural radioactivity in building materials vary significantly. Hence, this causes an excess indoor ^{222}Rn and it is calculated using Eq. (6) [2, 31, 32]:

$$C_{\text{Rn}} = \frac{U}{\lambda_v V}, \quad (6)$$

where U is the rate of radon entry into the room from building materials (Bq h^{-1}) and it is given as [2, 31]

$$U = \lambda P C_{\text{Ra}} \rho d A, \quad (7)$$

where λ_v and λ are the decay constants of radon (h^{-1}) and air exchange rate (h^{-1}), respectively. V is the room volume (m^3), P is the emanation fraction which was calculated previously, ρ is the density of the materials (kg m^{-3}), and d and A are the wall half-thickness (m) and exhaling area (m^2), respectively. A standard room with dimensions $4 \text{ m} \times 5 \text{ m} \times 2.8 \text{ m}$ and an air exchange rate of 0.5 h^{-1} was assumed. The thickness of the wall and density of the building were 20 m and 2400 kg m^{-3} , respectively. On the other hand, the volumes of the room and exhaling area are 56 m^3 and 20 m^2 , respectively.

The natural activity concentrations of various building materials were measured and analyzed using gamma-ray spectroscopy. The geometric mean activity concentration of each of the building materials under study is presented in Table 1 with values ranging from 10 ± 1 to 223 ± 5 , 9 ± 1 to 274 ± 8 , and 46 ± 7 to $1589 \pm 21 \text{ Bq kg}^{-1}$ for

^{226}Ra , ^{232}Th , and ^{40}K , respectively. On the other hand, to evaluate the contribution of building materials to the indoor environment, a standard room with an air exchange rate of 0.5 h^{-1} was assumed as mentioned above. The variation of the indoor radon concentration (^{222}Rn) from various building materials is presented in Fig. 3 with values ranging from 2.2 ± 0.1 to $54.9 \pm 1.3\text{ Bq m}^{-3}$ and a geometric mean of $10 \pm 9\text{ Bq m}^{-3}$. However, the geometric mean of ^{222}Rn of each of the building materials is also presented in Table 1. It can be observed that the activity concentrations and ^{222}Rn vary significantly among the building materials.

The highest activity concentrations of ^{226}Ra and ^{232}Th were obtained in the tile compared with other building materials under study and can be associated with ^{226}Ra and ^{232}Th contents of some of the tile raw materials such as feldspar, kaolin, and clay as shown in Table 1. However, ^{40}K is the most abundant radioactive element in nature: It can be found in water, brines, and some other minerals such as carnallite, feldspar, saltpeter, sylvite, and greensand. It is also an essential constituent of fertile soil and nutrients for plant growth and the human diet [33]. Therefore, it may not be surprising to find an elevated activity concentration of ^{40}K in some building materials such as pottery stone, glaze, and gravel. According to United Nations Scientific Committee on the Effects of Atomic Radiation (UNSCEAR) [34], the ^{226}Ra content of the building materials establishes the source of the radon emanation. High indoor ^{222}Rn may be found in buildings constructed using building materials with high ^{226}Ra

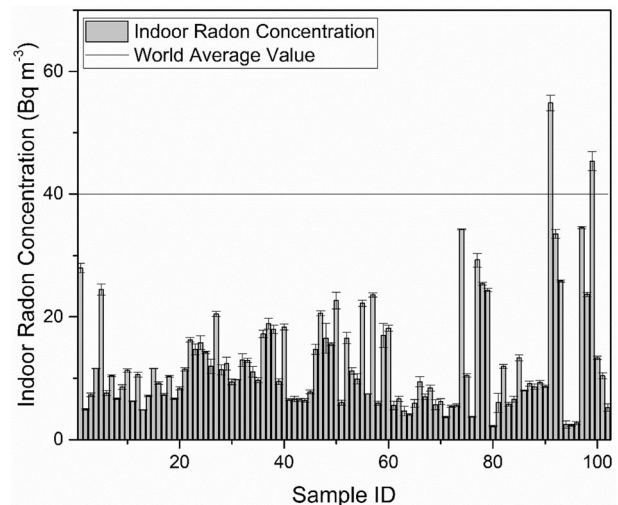


Fig. 3 Indoor radon concentration and world average value

content, although it also depends on other factors such as ventilation, porosity, radon emanation fraction, texture, density, permeability, and other environmental conditions that may influence the indoor ^{222}Rn levels in a room [34]. An example of the role of radon emanation fraction on ^{222}Rn level is shown in Table 1. It can be seen that tile has the highest ^{226}Ra content compared with sand and gravel, but the emanation fraction of tile is low. Hence, the ^{222}Rn level of sand and gravel is greater than that of tile.

UNSCEAR [35] reported the activity concentrations of the Malaysia's soils with mean values of 67, 82, and 310 Bq kg^{-1} for ^{226}Ra , ^{232}Th , and ^{40}K , respectively [35].

Table 1 Geometric mean of natural radioactivity and indoor radon concentration

Building materials	No. of samples	^{226}Ra (Bq kg^{-1})	^{232}Th (Bq kg^{-1})	^{40}K (Bq kg^{-1})	^{222}Rn (Bq m^{-3})
Tile	40	85 ± 40	65 ± 25	649 ± 220	11.0 ± 5.1
Red brick	5	33 ± 3	55 ± 8	505 ± 135	6.8 ± 0.6
Cement brick	5	46 ± 9	59 ± 15	576 ± 158	17.8 ± 3.5
Sand	10	38 ± 20	40 ± 20	358 ± 355	12.3 ± 6.6
Cement	10	28 ± 7	30 ± 9	194 ± 71	6.2 ± 1.6
Gravel	10	49 ± 64	45 ± 47	612 ± 475	9.5 ± 12.4
White cement	5	33 ± 15	35 ± 15	119 ± 12	8.2 ± 3.6
Fly ash	5	35 ± 2	34 ± 2	407 ± 21	8.7 ± 0.5
Feldspar	3	147 ± 61	58 ± 20	698 ± 329	36.2 ± 15.0
Limestone	3	10 ± 1	11 ± 3	60 ± 19	2.5 ± 0.2
Kaolin	1	140 ± 1	274 ± 8	703 ± 65	34.5 ± 0.2
Pottery stone	1	96 ± 2	54 ± 1	1114 ± 20	23.7 ± 0.4
Clay	2	100 ± 92	125 ± 72	533 ± 88	24.6 ± 22.7
Glaze	1	42 ± 2	51 ± 5	891 ± 1	10.4 ± 0.5
Talc	1	21 ± 3	36 ± 3	123 ± 13	5.2 ± 0.6
Geometric mean	102	53 ± 48	49 ± 37	441 ± 325	10 ± 9

Jang et al. [36] reported the indoor exposure caused by building materials using an HPGe detector and inductively coupled plasma mass spectrometry (ICP-MS) with mean values 57, 39, and 323 Bq kg⁻¹ for ²²⁶Ra, ²³²Th, and ⁴⁰K, respectively [36]. Ge and Zhang [37] reported the natural radioactivity concentration and associated radiological risks from building materials using gamma-ray spectroscopy. The average results are 39, 47, and 563 Bq kg⁻¹ for ²²⁶Ra, ²³²Th, and ⁴⁰K, respectively. These findings are in agreement with the results reported in our study.

Herein, we reported the study and the comparison of the indoor ²²²Rn concentration from some selected countries across Africa, Asia, Europe, and the Middle East. And the results, as shown in Table 2, showed that in Africa, the reported indoor ²²²Rn from Sudan, which is about 19 times higher than the value reported in our study, has exceeded the recommended level of 100 to 300, 200, and 200 to 600 set by WHO, EC, and ICRP level [1, 3, 11]. However, the average value is less than the action level of WHO and ICRP [3, 11]. On the other hand, the difference in the average values reported from Nigeria, Egypt, and Ghana is insignificant compared with the values obtained from our

study (about three times greater). They are less than the representative value of 40 Bq m⁻³ [11, 35]. In Asia, the values reported from India and Korea are approximately the same with the value reported in our study; however, the values reported from Japan and Thailand are 35% greater than the value reported in our study [38–40]. In the European site, though the reported indoor ²²²Rn from Cyprus and Lithuania is comparable to the values obtained from our study, our value is, however, 17 and 6 times smaller than the reported values from Bulgaria and Romania, respectively [41–44]. The indoor ²²²Rn reported in our study is about three and two times less than the values reported from Saudi Arabia and Kuwait, respectively [45, 46]. While the values from Turkey [47] are about eight times greater than our values, our values are greater than those reported from Yemen by four times [48].

Generally, if the world average value (40 Bq m⁻³) is taken as a reference value in the comparison, the indoor ²²²Rn reported is comparable with the values reported from Nigeria, Ghana, India, Korea, Japan, Thailand, Cyprus, Lithuania, Kuwait, Saudi Arabia, and Yemen; based on the world average value, the value reported is similar with 11

Table 2 Comparison of indoor ²²²Rn concentration with other published results from different parts of the world

Country	²²² Rn (Bq m ⁻³)	Techniques	Source
Africa			
Egypt	44 (15–132)	LR-115 Type II	[50]
Ghana	35 (11–111)	LR-115 Type II	[51]
Nigeria	39 (5–255)	CR-39	[52]
Sudan	245 (128–506)	CR-39	[53]
Asia			
India	16 (9–23)	LR-115 Type II	[54]
Japan	20 (3–125)	Alphaguard	[40]
Korea	13 (0–88) and 71 (7–572)	HPGe and ATD	[36, 55]
Thailand	20 (10–48)	IC	[38, 39]
Europe			
Bulgaria	227 (20–1117)	LR-115 Type II	[41]
Cyprus	19 (4–100)	CRM	[42]
Lithuania	14 (7–19)	Alphaguard	[43]
Romania	83	CR-39	[44]
Middle East/Western Asia			
Kuwait	25 (6–78)	Alphaguard	[45]
Saudi Arabia	36 (21–52)	CR-39	[46]
Turkey	98 (39–405)	LR-115 Type II	[47]
Yemen	3 (1–5)	CR-39	[48]
Representative values and present study			
World average value	40		[35]
Malaysia average value	14		[35]
Malaysia	13 (2–55)		Present study

CR-39 and LR-115 Type II are alpha track detectors, CRM is the continuous radon monitor, IC is the ionization chamber, and PT-DM is the passive-type radon/thoron descriptive monitor (Rn monitor)

out of 16 studies under comparison corresponding to 70% of the studies under comparison. The variation observed with other studies may be due to the geological variables of the materials beneath the dwellings, the type of building materials used in the construction, geographical condition, and atmospheric variables such as temperature and pressure differences [49]. Other factors that may lead to the variation include ventilation and radon emanation fraction. Therefore, the indoor ²²²Rn concentration reported in our study is in accordance with published results from various parts of the world.

3.3 Radiological risks analysis

The main contributions of the radiation dose received by the general public are originated from ²²⁶Ra, ²³²Th, and ⁴⁰K release mainly from building materials. Many countries have established guidelines to restrict the amount of natural radionuclides in building materials [13]. European Commission (EC) and IAEA showed that guidelines for building materials are primarily based on the activity concentration index (ACI) to the natural radionuclides of ²²⁶Ra, ²³²Th, and ⁴⁰K in the building materials [1, 13]. ²²⁶Ra content criterion should be added to the building materials with high emanation fraction [13]. To investigate the compliance of guidelines for the EC member states, the exemption level and upper level of ACI were given as 0.5 (exemption level) and 1 (upper level) for the building materials used in bulk quantities such as brick, cement, sand and gravel. While those of ACI were given as 2 (exemption level) and 6 (upper level) for the limited used building materials such as tiles or ceramic materials and board [1]. The exemption level and upper level of ACI are equivalent to 0.3 (exemption level) and 1 mSv y⁻¹ (upper level) from external exposure to γ-radiation, which is called an indoor annual effective dose (AED_{in}) in this study [1, 13]. The ACI and AED_{in} expressions are given in Eq. (8) and (10), respectively [1, 31, 35]. To determine AED_{in}, an indoor air-absorbed dose rate (D_{in}) must be estimated at 1 m above the ground surface by applying the conversion factors 0.92, 1.1, and 0.08 for ²²⁶Ra, ²³²Th, and 40 K as initiated by EC and given in Eq. (9) [1]:

$$ACI = \frac{C_{Ra}}{300} + \frac{C_{Th}}{200} + \frac{C_K}{3000} \tag{8}$$

$$D_{in} (nGy h^{-1}) = 0.92C_{Ra} + 1.1C_{Th} + 0.081C_K \tag{9}$$

$$AED_{in} (mSv y^{-1}) = 4.91 \times 10^{-3} (Sv h Gy^{-1}) \times D_{in} (nGy h^{-1}), \tag{10}$$

where C_{Ra}, C_{Th}, and C_K were previously defined. The calculated D_{in} was converted into AED_{in} using a conversion factor of 0.7 Sv Gy⁻¹ and other relevant parameters such as indoor time fraction (0.8 × 8765 h). Multiplying

0.7 Sv Gy⁻¹ by 7012 gives the multiplying factor 4908 Sv Gy⁻¹ h in Eq. (7). The multiplying factor was derived based on the assumption that an individual spent 80% of their indoors.

The variations in the ACI, D_{in} and AED_{in} are presented in Figs. 4 and 5. The calculated values range from 0.1 ± 0.01 to 2.1 ± 0.1, 22 ± 2 to 494 ± 12 nGy h⁻¹, and 0.1 ± 0.01 to 2.4 ± 0.6 mSv y⁻¹ with geometric mean values of 0.6 ± 0.4, 144 ± 97 nGy h⁻¹, and 0.7 ± 0.5 mSv y⁻¹ for ACI, D_{in}, and AED_{in}, respectively. It would be observed that from Fig. 4, almost all calculated ACI vales are below the recommended maximum value for building materials used in bulk quantity except for some ceramic raw materials such as feldspar, kaolin, and clay which slightly exceeded the recommended maximum value of 1. However, these ceramic raw materials are in the region of limited used building materials and therefore based on their criteria, they are all below the exemption level of 2. Figure 5a shows the variation of D_{in} across various building materials, and most of the values are above the world average value of 84 nGy h⁻¹. Though, according to an UNSCEAR report [35], Malaysia is among the countries with high D_{in} from the building materials [35]. Therefore, it may not be surprising to obtain high values of D_{in} in the current study. Additionally, the calculated values of AED_{in} shown in Fig. 5b indicated that almost all the main building materials are below the recommended maximum value of 1 mSv y⁻¹ except for tile, feldspar, kaolin, pottery stone, and clay which are slightly higher than 1 mSv y⁻¹. Therefore, the ceramic raw materials are the major contributors of the high-level radiation dose observed in the tile. One of the latest studies entitled

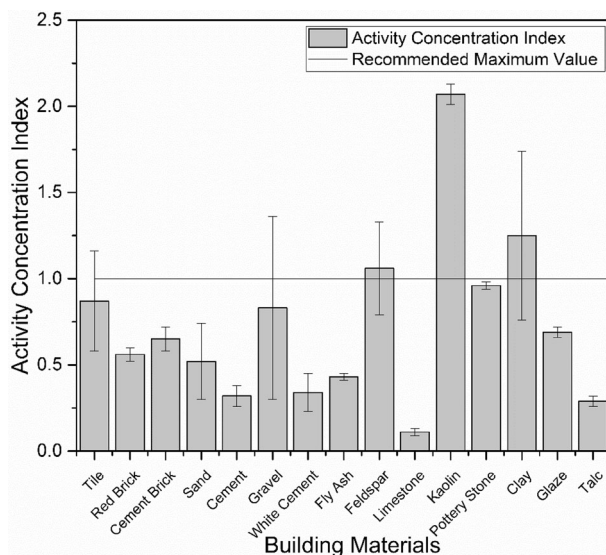


Fig. 4 Activity concentration index and recommended maximum value

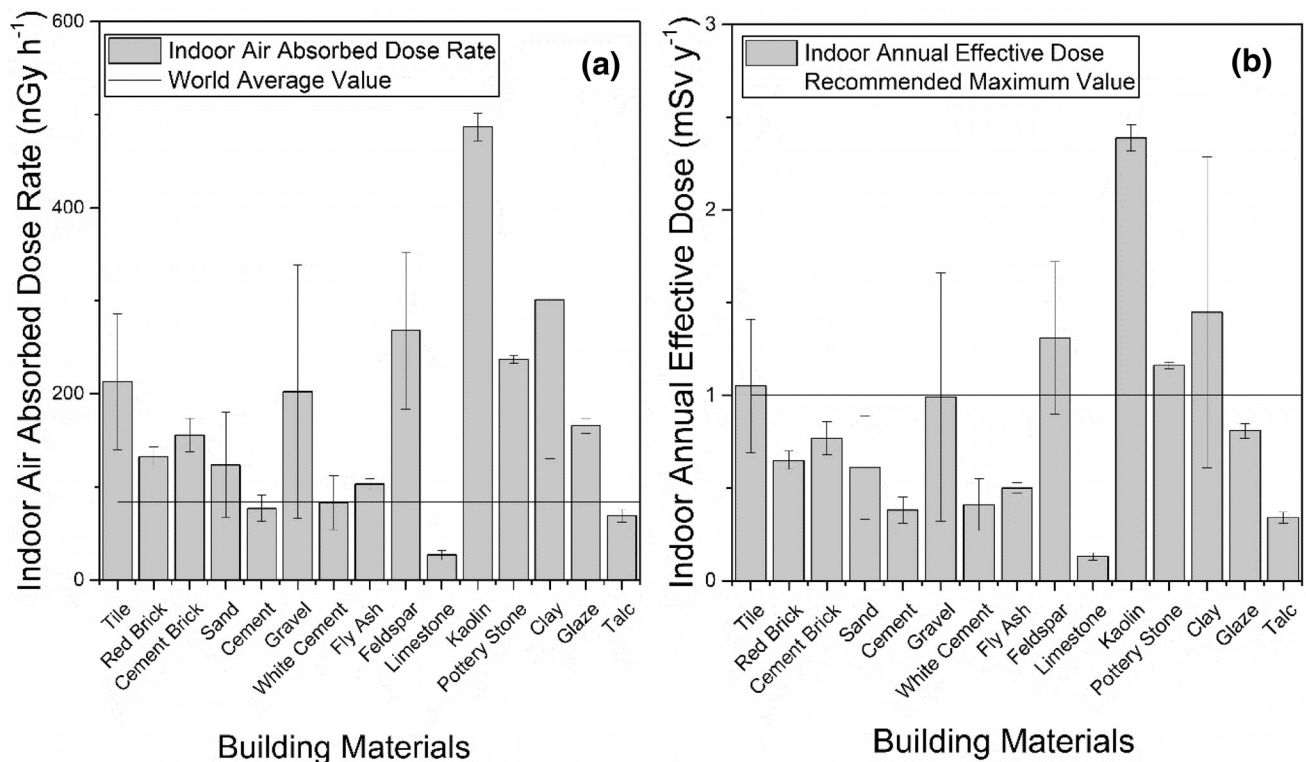


Fig. 5 (a) Indoor air absorbed dose rate and world average value and (b) annual effective dose and recommended maximum value

“Use of NORM-Containing Products in Construction” reported by Schroeyers et al. [56] focused on the building materials originated from industrial by-products from various countries around the world. The ACI for coal fly ash reported in their results is 0.8, while for ceramic, it ranges from 0.3 (Italy) to 1.9 (China) [56]. The average ACI for fly ash reported herein is 0.4, and for ceramic, it ranges from 0.1 (limestone) to 2.1 (kaolin). Despite this, the highest value reported in the present study is higher than the value reported from China, but still about 90% of our reported values are within the range stated from various countries in the study [56].

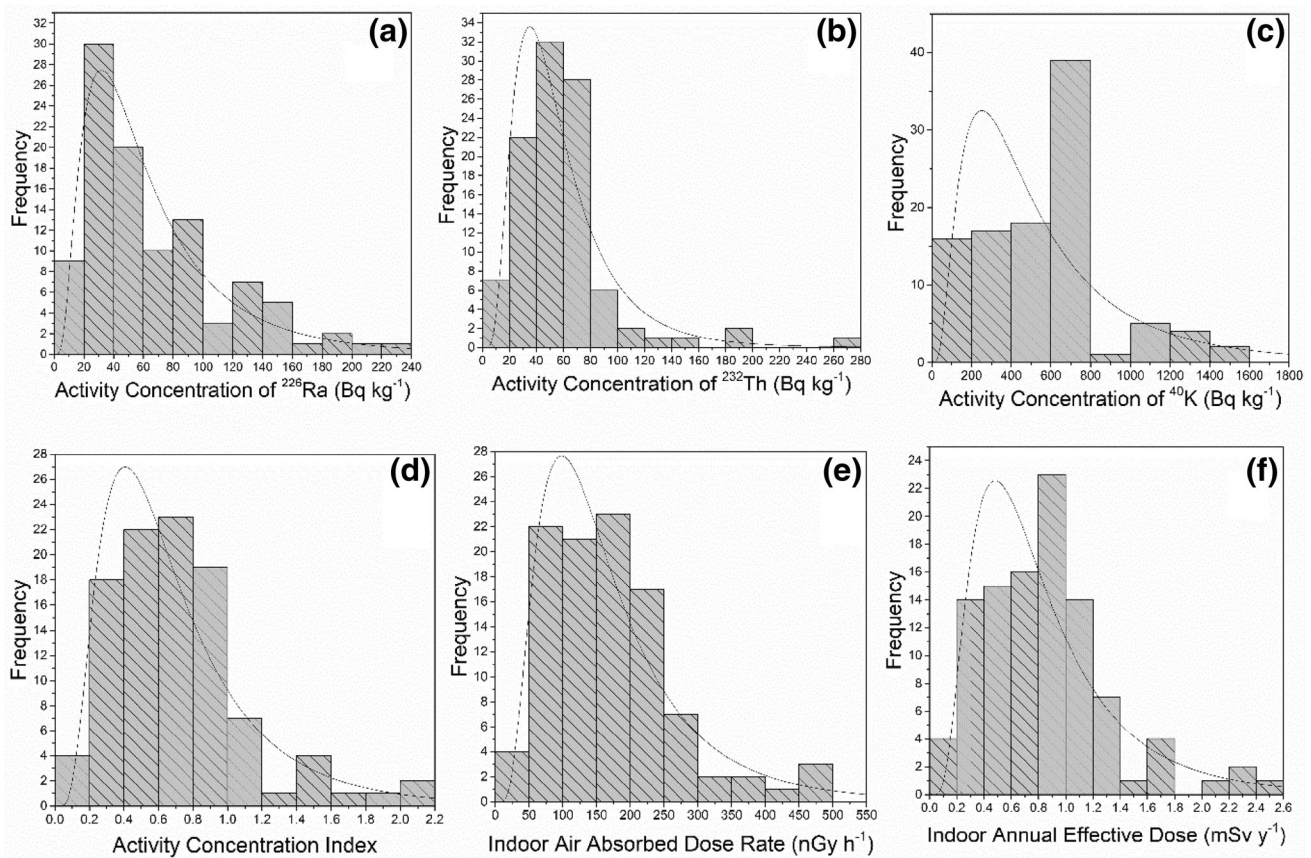
3.4 Statistical analysis of activity concentrations and radiological risk variables

The frequency distribution histogram, stem-and-leaf plot, P - P plot, and Q - Q plot are employed for visual normality examination. In this study, we employed frequency distribution histograms in addition to numerical tests such as the Shapiro–Wilk test (S - W test), Anderson–Darling test (A - D test), and Lilliefors test or modified Kolmogorov–Smirnov test (K - S test). The numerical tests of the activity concentrations and radiological risk parameters showed that the data were not significantly

drawn from the normally distributed population as shown in Table 3. The frequency distribution histograms of the activity concentrations of ²²⁶Ra, ²³²Th, and ⁴⁰K are shown in Fig. 6a–c, respectively, while the frequency distribution histograms of ACI, D_{in} , and AED_{in} are shown in Fig. 6d–f, respectively. The frequency distributions of the aforementioned parameters indicated that none of the parameters are normally distributed. Furthermore, for data to be normally distributed or drawn from the normal distribution, skewness and kurtosis of the data have to be zero or very close to zero. When the skewness is positive, this indicates the data are right-handed skewed, or if it is negative, it indicates the data are left-handed skewed. Similarly, positive kurtosis indicates a heavy tail or outliers and negative kurtosis indicates light tail or low outliers. The activity concentrations and radiological risk parameters showed positive skewness and kurtosis as shown in Table 3. Furthermore, the numerical tests including the S - W test, A - D test, and K - S test in addition to skewness and kurtosis indicate that the activity concentrations of ²²⁶Ra, ²³²Th, and ⁴⁰K and radiological risk parameters are asymmetrically distributed. The frequency distribution histograms were then compared with a lognormal curve, and it was found that most of the parameters fit the lognormal distribution curve while some few parameters such as ⁴⁰K and

Table 3 Statistical parameters of activity concentrations and radiological risk parameters

Statistical variables	^{226}Ra (Bq kg $^{-1}$)	^{232}Th (Bq kg $^{-1}$)	^{40}K (Bq kg $^{-1}$)	ACI	D_{in} (nGy h $^{-1}$)	AED $_{\text{in}}$ (mSv y $^{-1}$)
Geometric mean	53	49	441	0.6	144	0.7
STD	48	37	325	0.4	97	0.5
Min	10	9	46	0.1	22	0.1
25th	32	37	304	0.4	99	0.5
Median	54	54	600	0.7	166	0.8
75th	90	68	690	0.8	207	1.0
Max	223	274	1589	2.1	494	2.4
Interquartile range	58	31	387	0.4	108	0.5
Skewness	1.2	2.8	0.8	1.3	1.2	1.2
Kurtosis	1.0	12.3	0.9	2.4	2.1	2.1
Goodness-of-fit tests for normality						
Shapiro–Wilk test	< 0.01	< 0.01	< 0.01	< 0.01	< 0.01	< 0.01
Anderson–Darling test	< 0.01	< 0.01	< 0.01	< 0.01	< 0.01	< 0.01
Lilliefors test	< 0.01	< 0.01	< 0.01	< 0.01	< 0.01	< 0.01

**Fig. 6** Frequency distribution histogram of activity concentrations and radiological risk parameters compared with log-normal curves

indoor annual effective dose were a partially fitted log-normal curve. Some researchers such as Do Carmo Leal and Da Costa Lauria [57], Ravisankar et al. [58], and

Ravisankar et al. [59] concluded that the activity concentration of ^{40}K is normally distributed in most of the earth materials including building materials.

3.5 Radiological health effect of indoor radon concentration

The radon mass exhalation rate (E_m) is defined as the release of radon activity per unit time from unit mass of the matrix if the sample thickness is ≤ 10 times the radon diffusion length in the medium. Therefore, E_m is referred to as the radon production rate in the pore volume. In practical cases, measured E_m from the samples is referred to as radon production rate in the pore volume. E_m can be written as [28]:

$$E_m = PC_{Ra}\lambda. \quad (11)$$

The equilibrium equivalent concentration (EEC) of radon corresponding to a non-equilibrium mixture of short-lived radon daughters in air is defined as the radon activity concentration in radioactive equilibrium with its short-lived progeny. The short-lived progeny has the same potential alpha (α) energy concentration as the actual non-equilibrium mixture to which EEC refers [60, 61]. The equilibrium factor (F) is the ratio of the entire potential α energy for the actual radon daughter concentrations to the entire potential α energy of the radon daughters which would be in equilibrium with radon concentration [61]. In most cases, the indoor F is assumed to be 0.4 when estimating dose parameters due to radon exposure [61]. The EEC is calculated by multiplying the calculated C_{Rn} by F [28]. EEC can be written as:

$$EEC = F \times C_{Rn}. \quad (12)$$

Generally, F is defined within the range from 0 to 1. Therefore, C_{Rn} would be always higher than the concentration of its decay daughters [62].

Indoor annual effective dose (E_{Rn}) is the total dose due to radon received by the dweller in a year, and it was estimated following UNSCEAR [35]. The following parameters: indoor equilibrium factor as 0.4, the indoor occupancy time as 7008 h, and dose conversion factor as 9 nSv (Bq h m^{-3}) $^{-1}$ were applied and can be written as:

$$E_{Rn} = C_{Rn} \times 2.523 \times 10^{-2} \text{mSv Bq}^{-1} \text{m}^3. \quad (13)$$

The radiological health effect of indoor radon concentration was assessed through E_m , EEC, and E_{Rn} , while the variation of E_m , EEC, and E_{Rn} is presented in Figs. 7, 8 and 9, respectively. The aforementioned parameters show a non-uniform variation across various building materials and even within materials of the same kind. The results range from 33 to 674 $\text{mBq kg}^{-1} \text{h}^{-1}$, 0.9 to 22 Bq m^{-3} , and 0.1 to 1.4 mSv y^{-1} for E_m , EEC, and E_{Rn} , respectively. The fractional contribution of each of the building materials under study is shown in Table 4. Over 98% of EEC and E_{Rn} reported herein are below the world average value of 16 Bq m^{-3} and 1 mSv y^{-1} , respectively [35, 63].

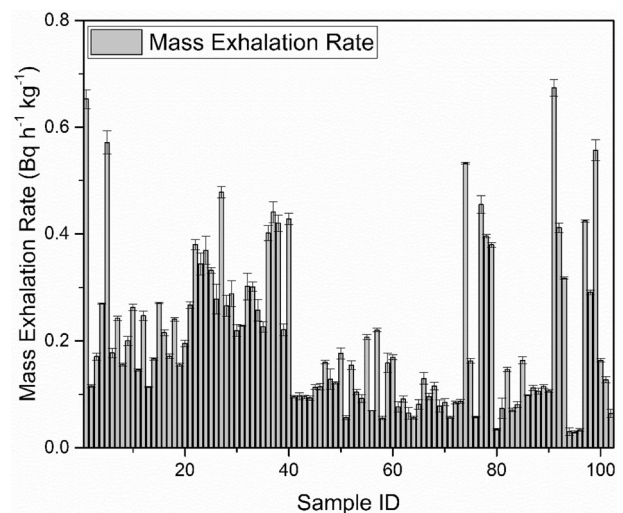


Fig. 7 Variation of mass exhalation rate

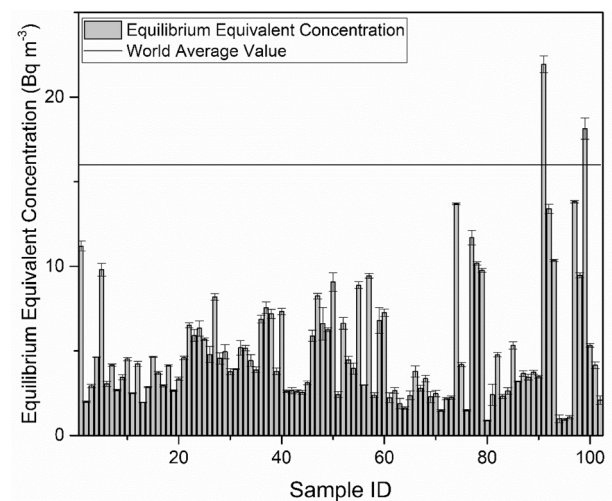


Fig. 8 Equilibrium equivalent concentration and world average value

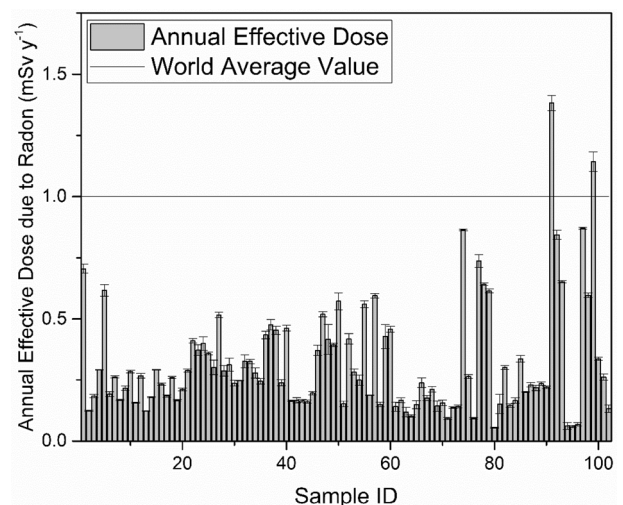


Fig. 9 Annual effective dose due to radon and its world average value

Table 4 Geometric mean of mass exhalation rate, equilibrium equivalent concentration, and annual effective dose due to radon

Building materials	No. of samples	E_m (mBq h ⁻¹ kg ⁻¹)	EEC (Bq m ⁻³)	E_{Rn} (mSv y ⁻¹)
Tile	40	258 ± 120	4.4 ± 2.1	0.3 ± 0.1
Red brick	5	98 ± 8	2.7 ± 0.2	0.2 ± 0.01
Cement brick	5	138 ± 27	7.1 ± 1.4	0.4 ± 0.1
Sand	10	115 ± 61	4.9 ± 2.6	0.3 ± 0.2
Cement	10	85 ± 22	2.5 ± 0.6	0.2 ± 0.04
Gravel	10	147 ± 193	3.8 ± 5.0	0.2 ± 0.3
White cement	5	100 ± 44	3.3 ± 1.4	0.2 ± 0.1
Fly ash	5	107 ± 6	3.5 ± 0.2	0.2 ± 0.01
Feldspar	3	445 ± 185	14.5 ± 6.0	0.9 ± 0.4
Limestone	3	31 ± 2	1.0 ± 0.1	0.1 ± 0.004
Kaolin	1	424 ± 2	13.8 ± 0.1	0.9 ± 0.004
Pottery stone	1	291 ± 5	9.5 ± 0.2	0.6 ± 0.01
Clay	2	302 ± 278	9.8 ± 9.1	0.6 ± 0.5
Glaze	1	127 ± 6	4.1 ± 0.2	0.3 ± 0.01
Talc	1	64 ± 8	2.1 ± 0.3	0.1 ± 0.02
Geometric mean	102	161 ± 144	4.1 ± 3.6	0.3 ± 0.2

Table 5 Comparison of annual effective dose due to inhalation of ²²²Rn with other published results from different parts of the world

Country	E_{Rn} (mSv y ⁻¹)	Techniques	Source
Africa			
Egypt	0.8 (0.6–0.9)	LR-115 type II	[50]
Ghana	1.2 (0.4–3.4)	LR-115 type II	[51]
Nigeria	1.9 (1.0–3.1) and 1.0	CR-39	[64]
Sudan	6.9 (3.6–14.2)	CR-39	[53]
Asia			
China	0.8	CR-39	[65]
India	0.5 (0.3–0.7)	LR-115 type II	[54]
Japan	0.4 (0.4–0.5) and 0.2	PT-DM	[40, 66]
Thailand	0.5 (0.3–1.2)	IC	[38, 39]
Europe			
Romania	2.4	LR-115 type II	[44]
Serbia	0.1	LR-115 type II	[67]
Middle East			
Saudi Arabia	0.6 (0.4–0.9)	CR-39	[46]
Turkey	5.1 (0.4 to 8.4)	CR-39	[68]
Yemen	0.06 (0.03–0.13)	CR-39	[48]
Representative value and present study			
World average value	1.0		[35]
Malaysia	0.3 (0.1–1.4)		Present study

CR-39 and LR-115 Type II are alpha track detectors, CRM is the continuous radon monitor, IC is the ionization chamber, and PT-DM is the passive-type radon/thoron descriptive monitor (Rn monitor)

To assess the exposure caused by ²²²Rn progeny, the EEC parameter plays a significant role in estimating the dose equivalent rate for organs and/or tissues such as lung and soft tissues. It can also be used to determine the effective dose equivalent when appropriate quality factors and dose coefficients are applied. However, E_{Rn} is one of

the reference indicators for the assessment of exposure caused by ²²²Rn and the results reported herein were all below the representative value [28, 35].

The compared annual effective dose due to inhalation of ²²²Rn is shown in Table 5. The comparison is based on the recently published studies from some selected countries in

Africa, Asia, Europe, and the Middle East. The results showed that most of the results can be compared with the results obtained from our study with the exception of results from Sudan, Turkey, and Romania which are relatively large compared with all other studies under comparison. Generally, the values in our results are only slightly higher than the values reported from Yemen and Serbia; otherwise, our result is compared with 77% of the reviewed literatures from the selected countries.

In general, the recommended exemption value of the annual effective dose due to inhalation of ^{222}Rn is 3 mSv y^{-1} while the action level is 10 mSv y^{-1} [3]. However, the representative value is 1 mSv y^{-1} which is equivalent to the indoor ^{222}Rn concentration of 40 Bq m^{-3} [35]. About 60% of the studies under comparison are below the representative value; however, only studies reported from Sudan and Turkey exceeded the exemption value which amount for 15% of the studies under comparison. Therefore, all studies including the value reported in our study are below the action level.

3.5.1 Dose equivalent rate for soft tissues (H_{ST}) and lung (H_L) and effective dose equivalent (H_{eff})

Radon is an inert noble gas which is not chemically bound in body tissues. However, the activity concentration of ^{222}Rn in the environmental air (EEC) is proportional to the activity concentration of ^{222}Rn in a tissue, T , due to its restricted saturation solubility. Inhaled ^{222}Rn is continuously present in the air volume of the lungs at the concentration in the environmental air which is partly dissolved in soft tissues. Moreover, the solubility factor is taken to be 0.4 for soft tissues and the short-lived daughters were assumed to decay in the same tissue as the parent ^{222}Rn gas. A quality factor of 20 for α radiation is applied for both soft tissues and lung, respectively [28, 60]. For equilibrium conditions, the dose equivalent rate for risk-relevant soft tissues is given as [60]:

$$H_{ST}(\text{nSv h}^{-1}) = 0.09 \times \text{EEC} (\text{Bq m}^{-3}). \quad (14)$$

In the case of the lungs, in addition to the dissolved ^{222}Rn , the air containing ^{222}Rn in the lung must be taken into account. The air volume in the lung is assumed to be $3.2 \times 10^{-2} \text{ m}^3$ for the reference man, and the short-lived decay products were assumed to stay in the lungs [28, 60]. The dose equivalent rate for the lung is [60]:

$$H_L (\text{nSv h}^{-1}) = 0.8 \times \text{EEC} (\text{Bq m}^{-3}). \quad (15)$$

Furthermore, applying the tissue weighing factor of 0.12 for lung and 0.88 for other risk-relevant tissues, an effective dose equivalent rate is given as [28, 60]:

$$H_{eff}(\text{nSv h}^{-1}) = 0.18\text{EEC}(\text{Bq m}^{-3}). \quad (16)$$

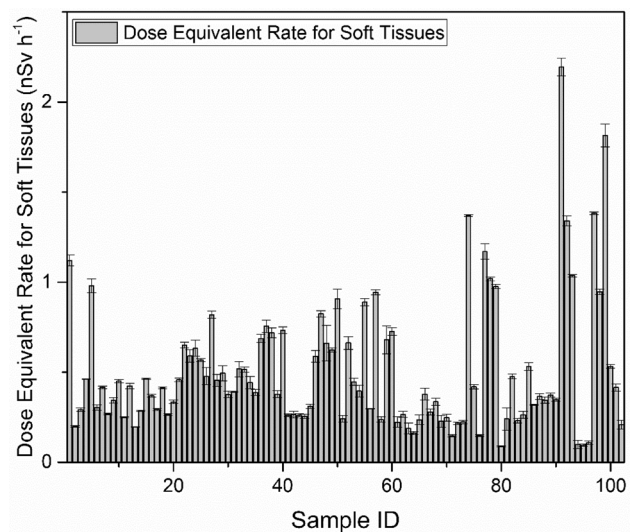


Fig. 10 Variation of dose equivalent rate for soft tissues

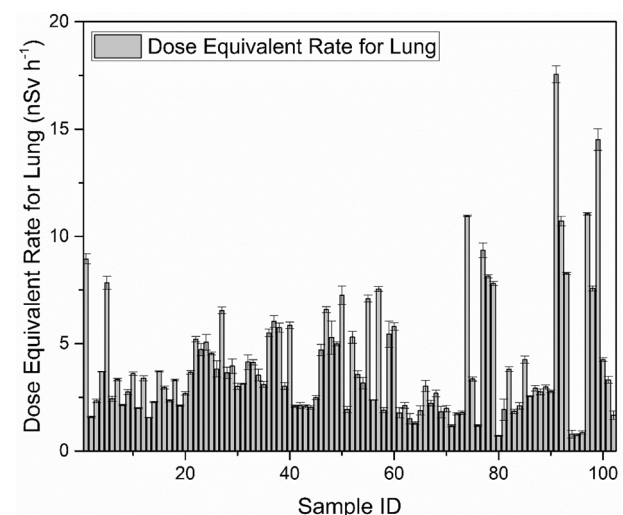


Fig. 11 Variation of dose equivalent rate for lung

The detailed derivation of Eqs. (14) to (15) is presented in the ICRP publication 32 [60] and UNSCEAR [28].

It is convenient to assess the doses from the inhalation of ^{222}Rn gas, since the gas is soluble in the body fluids and tissues, and it can be easily transported all over the body. With this, doses would be delivered from decay of the gas itself and its short-lived decay daughters [63]. Therefore, the fractional contribution of dose equivalent rates for soft tissues (H_{ST}) and lung (H_L) and effective dose equivalent (H_{eff}) were scrutinized. The variations of the calculated doses are presented in Figs. 10, 11 and 12, with values ranging from 0.1 ± 0.01 to 2.2 ± 0.1 , 0.7 ± 0.03 to 17.6 ± 0.4 , and 0.2 ± 0.01 to $4.0 \pm 0.1 \text{ nSv h}^{-1}$ for H_{ST} , H_L , and H_{eff} , respectively. On the other hand, the contributions of each of the building materials are presented in

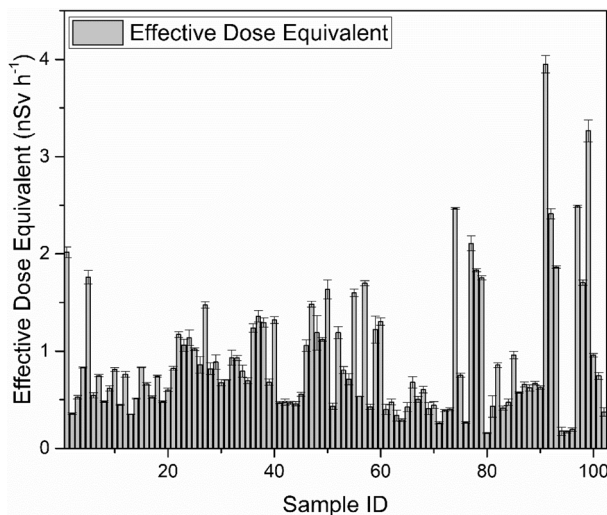


Fig. 12 Variation of effective dose equivalent

Table 6 Geometric mean of dose equivalent rates for soft tissues and lung and effective dose equivalent

Building materials	No. of samples	H_{st} (nSv h ⁻¹)	H_L (nSv h ⁻¹)	H_{eff} (nSv h ⁻¹)
Tile	40	0.4	3.5	0.8
Red brick	5	0.3	2.2	0.5
Cement brick	5	0.7	5.7	1.3
Sand	10	0.5	3.9	0.9
Cement	10	0.2	2.0	0.4
Gravel	10	0.4	3.0	0.7
White cement	5	0.3	2.6	0.6
Fly ash	5	0.3	2.8	0.6
Feldspar	3	1.4	11.6	2.6
Limestone	3	0.1	0.8	0.2
Kaolin	1	1.4	11.1	2.5
Pottery stone	1	0.9	7.6	1.7
clay	2	1.0	7.9	1.8
Glaze	1	0.4	3.3	0.7
Talc	1	0.2	1.7	0.4
Geometric mean	102	0.4 ± 0.4	3.3 ± 2.9	0.7 ± 0.7

Table 6, and it can be seen that the variations of the doses are not uniform throughout the building materials. In other words, each building material has a unique fractional contribution to the doses received by an individual. The H_L values reported herein from all building materials were all greater than the representative value of 0.8 nSv h⁻¹ while over 85% of the H_{ST} reported herein were below the representative value of 1.2 nSv h⁻¹ [63].

4 Conclusion

In this study, the activity concentrations of ²²⁶Ra, ²³²Th, and ⁴⁰K in various building materials were measured using gamma-ray spectroscopy coupled with an HPGe detector. The activity concentrations were further evaluated for probable radiological health hazards by assessing ACI, D_{in} , and AED_{in} with results ranging from 0.1 ± 0.01 to 2.1 ± 0.1, 22 ± 2 to 494 ± 12 nGy h⁻¹, and 0.1 ± 0.01 to 2.4 ± 0.6 mSv y⁻¹, respectively. The calculated P and ²²²Rn values range from 10.0 ± 0.4 to 30.0 ± 0.4% and 2.2 ± 0.1 to 54.9 ± 1.3 Bq m⁻³, respectively. On the other hand, E_m , EEC, and E_{Rn} were computed and the results range from 33 to 674 mBq h⁻¹ kg⁻¹, 0.9 to 22 Bq m⁻³, and 0.1 to 1.4 mSv y⁻¹, respectively. The internal doses caused by inhalation of radon and its progeny were also estimated, and the results range from 0.1 ± 0.01 to 2.2 ± 0.1, 0.7 ± 0.03 to 17.6 ± 0.4, and 0.2 ± 0.01 to 4.0 ± 0.1 nSv h⁻¹ for H_{ST} , H_L , and H_{eff} , respectively. The reported results for external dose (AED_{in}) and internal dose (E_{Rn}) were below the recommended maximum limit of 1 and 10 mSv y⁻¹, respectively. The results reported herein are in agreement with other previous studies including representative values reported by international organizations dealing with radiation protection. Therefore, the radiological health risks attributed to the building materials under study are negligible. However, different individuals may have a different tolerance to the radiation exposure and there is no specific level below which the indoor radon level may be considered safe.

Acknowledgements The authors would like to acknowledge all laboratory technicians of the Nuclear Science Program, UKM, for their technical support throughout the works. Shittu Abdullahi also wishes to appreciate and acknowledge Gombe State University, Gombe, Nigeria, for providing the Ph.D fellowship.

References

1. EC, Radiation Protection 112: Radiological Protection Principles concerning the Natural Radioactivity of Building Materials, Finland (1999), <https://ec.europa.eu/energy/sites/ener/files/documents/112.pdf>. Accessed 20 July 2017
2. NEA-OECD, Exposure to Radiation from Natural Radioactivity in Building Materials (1979), pp. 1–34. <https://www.oecd-nea.org/rp/reports/1979/exposure-to-radiation-1979.pdf>
3. ICRP Publication 65, Protection against radon-222 at home and at work. A report of a task group of the international commission on radiological protection (ICRP Publication 65, PERGAMON, 1993)
4. ICRP Publication 115, Lung Cancer Risk from Radon and Progeny and Statement on Radon (2010). <https://doi.org/10.1016/j.icrp.2011.08.011>
5. S. Abdullahi, A.F. Ismail, S.B. Samat et al., Assessment of natural radioactivity and associated radiological risks from tiles used

- in Kajang, Malaysia. *Am Inst Phys* **1940**(020001), 1–6 (2018). <https://doi.org/10.1063/1.5027916>
6. A.D. Bajoga, N. Alazemi, P.H. Regan et al., Radioactive investigation of NORM samples from Southern Kuwait soil using high-resolution gamma-ray spectroscopy. *Radiat. Phys. Chem.* **116**, 305–311 (2015). <https://doi.org/10.1016/j.radphyschem.2015.01.041>
 7. A.A. Safarov, A.N. Safarov, A.N. Azimov et al., Rapid assessment methodology in NORM measurements from building materials of Uzbekistan. *J. Environ. Radioact.* **169**, 186–191 (2017). <https://doi.org/10.1016/j.jenvrad.2017.01.019>
 8. K. Yuvi, Indoor air quality: radon report on a WHO Working. *J. Environ. Radioact.* **8**, 73–91 (1988)
 9. M. Kaur, A. Kumar, R. Mehra et al., Study of radon/thoron exhalation rate, soil-gas radon concentration, and assessment of indoor radon/thoron concentration in Siwalik Himalayas of Jammu & Kashmir. *Hum. Ecol. Risk Assess. Int. J.* (2018). <https://doi.org/10.1080/10807039.2018.1443793>
 10. Ö. Karadeniz, G. Günalp, T. Özbay et al., Preliminary dose estimation from indoor radon for the medical staff of Radiation Oncology and Nuclear Medicine. *Hum. Ecol. Risk Assess. Int. J.* **22**(7), 1574–1582 (2016). <https://doi.org/10.1080/10807039.2016.1202084>
 11. WHO, WHO Handbook on Indoor Radon: A Public Health Perspective, World Health Organization (2009). <http://www.nrsb.org/pdf/WHORadonHandbook.pdf>. Accessed 29 Sept 2017
 12. US NTP, 14th Report on Carcinogens (Ionizing Radiation) (2016). <https://ntp.niehs.nih.gov/ntp/roc/content/profiles/ionizingradiation.pdf>. Accessed 24 May 2018
 13. IAEA, Protection of the public against exposure indoors due to radon and other natural sources of radiation, Vienna (2015). <https://www-pub.iaea.org/MTCD/Publications/PDF/Pub1651Web-62473672.pdf>. Accessed 24 May 2018
 14. IARC, Evaluation of the Carcinogenic Risks to Humans, Lyon (1988). <http://monographs.iarc.fr/ENG/Monographs/vol43/mono43.pdf>. Accessed 24 May 2018
 15. E. Abuelhia, Evaluation of annual effective dose from indoor radon concentration in Eastern Province, Dammam, Saudi Arabia. *Radiat. Phys. Chem.* **140**, 137–140 (2017). <https://doi.org/10.1016/j.radphyschem.2017.03.004>
 16. S. Sun, J.H. Schiller, A.F. Gazdar, Lung cancer in never smokers—a different disease. *Nat. Rev. Cancer* **7**, 778–790 (2007). <https://doi.org/10.1038/nrc2190>
 17. M. Torres-Durán, J.M. Barros-Dios, A. Fernández-Villar et al., Residential radon and lung cancer in never smokers. A systematic review. *Cancer Lett.* **345**, 21–26 (2014). <https://doi.org/10.1016/j.canlet.2013.12.010>
 18. MNCR, Malaysian National Cancer Registry Report 2007–2011, Putrajaya (2016). <http://nci.moh.gov.my>
 19. M. Pérez-Ríos, J.M. Barros-Dios, A. Montes-Martínez et al., Attributable mortality to radon exposure in Galicia, Spain. Is it necessary to act in the face of this health problem? *BMC Public Health.* **10**, 256–262 (2010). <http://www.biomedcentral.com/1471-2458/10/256>. Accessed 26 May 2018
 20. IAEA, Measurement of Radionuclides in Food and the Environment, IAEA, Vienna (1989). http://www-pub.iaea.org/MTCD/Publications/PDF/trs295_web.pdf. Accessed 10 Oct 2017
 21. ADVANCETECH, High-purity Germanium (HPGe) Detectors, Adv. Technol. Gr. <https://www.advantech.in/hpge-detector>. Accessed 18 May 2018
 22. M.S. Yasir, A.A. Majid, R. Yahaya, Study of natural radionuclides and its radiation hazard index in Malaysian building materials. *J. Radioanal. Nucl. Chem.* **273**(3), 539–541 (2007). <https://doi.org/10.1007/s10967-007-0905-7>
 23. CANBERRA. Spectrum Analysis (Mirion Technologies, 2010). <http://www.canberra.com/literature/fundamental-principles/pdf/Spectrum-Analysis.pdf>. Accessed 7 Apr 2018
 24. K.F. Jamil, S. Ali, H.A. Khan, Determination of equilibrium factor between radon and its progeny using surface barrier detector for various shapes of passive radon dosimeters. *Nucl. Instrum. Methods A* **388**, 267–272 (1997)
 25. IAEA, Measurement and Calculation of Radon Releases from NORM Residues, Vienna (2013)
 26. A. Sakoda, Y. Nishiyama, K. Hanamoto et al., Differences of natural radioactivity and radon emanation fraction among constituent minerals of rock or soil. *Appl. Radiat. Isot.* **68**, 1180–1184 (2010). <https://doi.org/10.1016/j.apradiso.2009.12.036>
 27. B.K. Sahoo, D. Nathwani, K.P. Eappen et al., Estimation of radon emanation factor in Indian building materials. *Radiat. Meas.* **42**, 1422–1425 (2007). <https://doi.org/10.1016/j.radmeas.2007.04.002>
 28. UNSCEAR, Sources, Effects and Risks of Ionising Radiation (Exposures from Natural Sources of Radiation), New York, 1988
 29. S.D.E. Martino, C. Sabbarese, G. Monetti, Radon emanation and exhalation rates from soils measured with an electrostatic collector. *Appl. Radiat. Isot.* **49**, 407–413 (1998)
 30. P. Bossew, The radon emanation power of building materials, soils and rocks. *Appl. Radiat. Isot.* **59**, 389–392 (2003). <https://doi.org/10.1016/j.apradiso.2003.07.001>
 31. M. Markkanen, Radiation Dose Assessments for Materials with Elevated Natural Radioactivity (1995). http://www.iaea.org/inis/collection/NCLCollectionStore/_Public/28/021/28021209.pdf
 32. A.F. Saad, R.M. Abdallah, N.A. Hussein, Radon exhalation from Libyan soil samples measured with the SSNTD technique. *Appl. Radiat. Isot.* **72**, 163–168 (2013)
 33. Argonne National Laboratory, Potassium-40 (2005). <http://phi.nmsu.edu/~pvs/teaching/phys593/potassium.pdf>. Accessed 13 May 2018
 34. UNSCEAR, Sources and Effects of Ionizing Radiation (Natural Sources of Radiation), New York (1977). http://www.unscear.org/docs/publications/1977/UNSCEAR_1977_Annex-B.pdf. Accessed 21 Jan 2018
 35. UNSCEAR, Sources and effects of ionizing radiation (Exposures from Natural Radiation Sources), New York, 2000
 36. M. Jang, K.H. Chung, Y.Y. Ji et al., Indoor external and internal exposure due to building materials containing NORM in Korea. *J. Radioanal. Nucl. Chem.* **307**, 1661–1666 (2016). <https://doi.org/10.1007/s10967-015-4375-z>
 37. J. Ge, J. Zhang, Natural radioactivity and radiation hazards of building materials in Anhui Province, China. *J. Radioanal. Nucl. Chem.* **304**, 609–613 (2015). <https://doi.org/10.1007/s10967-014-3891-6>
 38. P. Sola, W. Srinuttrakul, S. Laoharajanaphand et al., Estimation of indoor radon and the annual effective dose from building materials by ionization chamber measurement. *J. Radioanal. Nucl. Chem.* **302**, 1531–1535 (2014). <https://doi.org/10.1007/s10967-014-3716-7>
 39. P. Sola, W. Srinuttrakul, P. Kewsuwan, Estimation of the indoor radon and the annual effective dose from granite samples. *J. Phys. Conf. Ser.* **611**, 012013 (2015). <https://doi.org/10.1088/1742-6596/611/1/012013>
 40. H. Tsuruoka, K. Inoue, S. Hosokawa et al., Measurement of radon and thoron concentrations in the Tokyo Metropolitan University Arakawa Campus building. *J. Jpn. Acad. Heal. Sci.* **19**, 40–48 (2016)
 41. K. Ivanova, Z. Stojanovska, M. Tsenova et al., Building-specific factors affecting indoor radon concentration variations in different regions in Bulgaria. *Air Qual. Atmos. Heal.* **10**(9), 1151–1161 (2017). <https://doi.org/10.1007/s11869-017-0501-0>

42. I. Sarrou, I. Pashalidis, Radon exhalation from granite counter-tops and expected indoor radon levels. *J. Radioanal. Nucl. Chem.* **311**, 913–916 (2017). <https://doi.org/10.1007/s10967-016-5108-7>
43. L. Pilkyte, D. Butkus, Influence of gamma radiation of indoor radon decay products on absorbed dose rate. *J. Environ. Eng. Landsc. Manag.* **13**, 65–72 (2005)
44. C. Cosma, K. Szacsvai, A. Dinu et al., Preliminary integrated indoor radon measurements in Transylvania (Romania). *Isot. Environ. Health Stud.* **45**, 259–268 (2009)
45. J. Al-Hubail, D. Al-Azmi, Radiological assessment of indoor radon concentrations and gamma dose rates in secondary school buildings in Kuwait. *Constr. Build. Mater.* **183**, 1–6 (2018). <https://doi.org/10.1016/j.conbuildmat.2018.06.152>
46. S.M. Farid, Indoor radon in dwellings of Jeddah city, Saudi Arabia and its correlations with the radium and radon exhalation rates from soil. *Indoor Built Environ.* **25**, 269–278 (2016). <https://doi.org/10.1177/1420326X14536749>
47. Z. Yasar, C. Taşköprü, M. İçhedef et al., Indoor radon levels of spas and dwellings located around Bayındır geothermal region. *J. Radioanal. Nucl. Chem.* **299**, 343–349 (2014). <https://doi.org/10.1007/s10967-013-2726-1>
48. M. Al Mugahed, F. Bentayeb, Radon exhalation from building materials used in Yemen. *Radiat. Prot. Dosim.* (2018). <https://doi.org/10.1093/rpd/ncy081>
49. L. Sahin, H. Cetinkaya, S. Gelgun, Assessment of annual effective dose due to the indoor radon exposure in a second-degree earthquake zone of Kutahya (Turkey). *Rom. J. Phys.* **61**, 687–696 (2016)
50. M. Abd-Elzaher, Measurement of indoor radon concentration and assessment of doses in different districts of Alexandria city, Egypt. *Environ. Geochem. Health* **35**, 299–309 (2013). <https://doi.org/10.1007/s10653-012-9494-7>
51. C.Y. Ansre, M.K. Miyittah, A.B. Andam et al., Risk assessment of radon in the South Dayi District of the Volta Region, Ghana. *J. Radiat. Res. Appl. Sci.* **11**, 10–17 (2018). <https://doi.org/10.1016/J.JRRAS.2017.10.002>
52. O.S. Ajayi, O.E. Olubi, Investigation of indoor radon levels in some dwellings of southwestern Nigeria. *Environ. Forensics* **17**, 275–281 (2016). <https://doi.org/10.1080/15275922.2016.1230909>
53. A.E.A. Elzain, Radon exhalation rates from some building materials used in Sudan. *Indoor Built Environ.* **24**, 852–860 (2015). <https://doi.org/10.1177/1420326X14537285>
54. M. Kumar, A. Agrawal, R. Kumar, Radiation dose due to radon, thoron and their decay products in indoor environment of Khurja City, U.P., India. *J. Radioanal. Nucl. Chem.* **300**, 39–44 (2014). <https://doi.org/10.1007/s10967-014-2946-z>
55. T.H. Park, D.R. Kang, S.H. Park et al., Indoor radon concentration in Korea residential environments. *Environ. Sci. Pollut. Res.* **1**, 5 (2018). <https://doi.org/10.1007/s11356-018-1531-3>
56. W. Schroevers, Z. Sas, G. Bator et al., Use of NORM-containing products in construction: the NORM4Building database, a tool for radiological assessment when using by-products in building materials. *Constr. Build. Mater.* **159**, 755–767 (2018). <https://doi.org/10.1016/j.conbuildmat.2017.11.037>
57. A.L. Da Costa Leal, D. Do Carmo Lauria, Assessment of doses to members of the public arising from the use of ornamental rocks in residences. *J. Radiol. Prot.* **36**, 680–694 (2016)
58. R. Ravisankar, K. Vanasundari, A. Chandrasekaran et al., Measurement of natural radioactivity in building materials of Namakkal, Tamil Nadu, India using gamma-ray spectrometry. *Appl. Radiat. Isot.* **70**, 699–704 (2012)
59. R. Ravisankar, K. Vanasundari, M. Suganya et al., Multivariate statistical analysis of radiological data of building materials used in Tiruvannamalai, Tamilnadu, India. *Appl. Radiat. Isot.* **85**, 114–127 (2014)
60. ICRP Publication 32, Limits for Inhalation of Radon Daughters by Workers, New York (1981). http://journals.sagepub.com/doi/pdf/10.1177/ANIB_6_1. Accessed 14 May 2018
61. UNSCEAR, Ionizing Radiation: Sources and Biological Effects (Exposures to Radon and Thoron and Their Decay Products), New York, 1982. http://www.unscear.org/docs/publications/1982/UNSCEAR_1982_Annex-D.pdf. Accessed 12 Oct 2017
62. M.Y.M. Ali, M.M. Hanafiah, M.F. Khan, Potential factors that impact the radon level and the prediction of ambient dose equivalent rates of indoor microenvironments. *Sci. Total Environ.* **626**, 1–10 (2018). <https://doi.org/10.1016/j.scitotenv.2018.01.080>
63. UNSCEAR, Sources and Effects of Ionizing Radiation (Exposure from Natural Sources of Radiation), New York, 1993. http://www.unscear.org/docs/publications/1993/UNSCEAR_1993_Annex-A.pdf. Accessed 29 Sept 2017
64. R.I. Obed, H.T. Lateef, A.K. Ademola, Indoor radon survey in a university campus of Nigeria. *J. Med. Phys.* **35**, 242–246 (2010). <https://doi.org/10.4103/0971-6203.71760>
65. L. Zhang, C. Liu, Q. Guo, Measurements of thoron and radon progeny concentrations in Beijing, China. *J. Radiol. Prot.* **28**, 603–607 (2008). <https://doi.org/10.1088/0952-4746/28/4/N02>
66. S. Oikawa, N. Kanno, T. Sanada et al., A survey of indoor workplace radon concentration in Japan. *J. Environ. Radioact.* **87**, 239–245 (2006). <https://doi.org/10.1016/j.jenvrad.2005.12.001>
67. P. Ujčić, I. Čeliković, A. Kandić et al., Internal exposure from building materials exhaling ²²²Rn and ²²⁰Rn as compared to external exposure due to their natural radioactivity content. *Appl. Radiat. Isot.* **68**, 201–206 (2010). <https://doi.org/10.1016/j.apradiso.2009.10.003>
68. M. Kıldır, İ. Gökmen, A. Gökmen, Indoor radon concentrations and radon doses at three districts of Ankara, Turkey and raising public awareness on the issue. *J. Radioanal. Nucl. Chem.* **307**, 777–786 (2016). <https://doi.org/10.1007/s10967-015-4489-3>